International Journal of GEOMATE, Aug. 2023, Vol. 25, Issue 108, pp.163-171
ISSN: 2186-2982 (P), 2186-2990 (O), Japan, DOI: https://doi.org/10.21660/2023.108.3798
Geotechnique, Construction Materials and Environment

UNDERSTANDING DOWNSTREAM SLOPE FAILURE IN EARTH DAMS: CAUSES AND REMEDIES - A CASE STUDY OF TRIEU THUONG NO.2 DAM, QUANG TRI, VIETNAM

The Viet Tran[1], *Thao Ba Vu[2], Minh Van Pham[3], Dung Quoc Nguyen[4], and Duong Cao Phan[2]

[1]Department of Civil Engineering, Thuyloi University, Vietnam
[2,5] Department of Geotechnical Engineering, Hydraulic Construction Institute, Vietnam Academy for Water Resources, Vietnam
[3]Central Project Office, Ministry of Agriculture and Rural Development, Vietnam
[4]Vietnam National Committee on Large Dams and Water Resources Development

*Corresponding Author, Received: 06 Feb. 2023, Revised: 09 April 2023, Accepted: 28 May 2023

ABSTRACT: Lessons learned from dealing with earth dam incidents have made a significant contribution to surveying, designing, constructing, and repairing works. However, disseminating these lessons to the public must be done carefully. This study aims to analyze the causes and remedial measures for the downstream failure of the Trieu Thuong No. 2 earthen dam in Quang Tri province, Vietnam. To achieve this, the finite element software, MIDAS, was used for seepage and slope stability analysis. The simulation was based on design documents, past responses to dam incidents, and additional geological survey data. The results indicated that there were three major causes of instability in the dam: (1) the existence of a soft soil layer beneath the upstream slope foundation that was not recognized in the original design; (2) a difference in hydraulic conductivity between the original dam soil and the backfill; and (3) the absence of a drainage arrangement between the new and original layers of the dam. Therefore, proposed solutions include (1) reducing settlement by reinforcing the foundation beneath the downstream slope with soil-cement columns; (2) using soil backfill with a higher permeability coefficient than the existing dam to expand the dam crest; and (3) implementing a drainage system between the new and old layers of the dam. These solutions have been found to address the problem of downstream slope instability and can serve as a reference for future projects.

Keywords: Earth dam, Soil-cement columns, Drainage system, Slope stability, MIDAS

1. INTRODUCTION

According to the state authority for construction quality inspection, there were around 7,000 dams in Vietnam in 2013, with approximately 675 classified as large and the rest as small or medium, with a dam height of fewer than 15 meters. The most common type of dam in Vietnam is the earth dam, which is the oldest form of embankment and can be constructed using local materials and simple equipment [1]. Many of the small and medium-sized earth dams in Vietnam were built between the 1960s and 1980s when surveying techniques were limited, construction equipment was outdated, and design standards were incomplete. As a result, greater attention has been focused on this type of dam, and further studies are needed to investigate the causes, mechanisms, and remedial measures for failures of earth dams.

Dam failures have occurred throughout history [2], raising significant concerns due to their economic and environmental impacts [2-5]. The instability of earth dams can be attributed to three primary categories of failure: hydraulic, seepage, and structural [6]. Research conducted by Lukman et al. [4] identified leakage and piping as the most common causes of dam failure at 35%, followed by overtopping at 25%, spillway erosion at 14%, and other reason such as excessive deformation (11%), sliding (10%), gate failure (2%), faulty construction (2%), and earthquake instability (2%). Arora's survey [7] also found that hydraulic failure accounted for 35% of dam failures, with seepage and structural failures accounting for 20-30% each and other causes accounting for the remaining 7%. Notably, earthen dams have a higher failure frequency than concrete dams, with reports showing a rate about four times greater. Therefore, greater emphasis should be placed on monitoring and improving the safety of earthen dams [5].

Analyzing about 900 cases of dam failures, Zhang, Xu, and Jia [8] found that overtopping and piping are the most common causes of earth dam failures. Managing uncontrolled seepage through the body and foundation of embankments is a major concern for engineers operating dams [9]. The seepage flow within hydraulic structures, like dams, has a significant impact on their stability and deformation [10-12]. Seepage might trigger slope failure by generating high pressure on the pores within the soil or by increasing the wetness of the slope. Inadequate seepage control measures or poor cleanup and preparation of foundations and abutments have resulted in many seepage problems and earth dam failures [13]. Uncontrolled or concentrated seepage through the dam may lead to piping through the dam body or foundation or sloughing of the downstream side and the subsequent failure of the dam [6, 9, 13]. Therefore, seepage assessment and analysis are critical components of dam and embankment design [9, 10].

Learning from past failures and damages is a crucial aspect of the training for earth dam designers [14]. Effective dam design requires the implementation of both preventive and mitigation measures [2]. Properly evaluating the cause of seepage and instability in a dam is necessary to select the right solution for troubleshooting. Common treatment methods involve grouting curtains, excavation of permeable materials, cutoff walls, and upstream impervious blankets to control seepage, which can result in significant savings in structure dimensions [9]. This study aims to examine the causes of downstream failure in the Trieu Thuong No. 2 earthen dam in Quang Tri province, Vietnam, and propose suitable remedial measures. Seepage and slope stability analysis were conducted using finite element software MIDAS, along with additional geological surveys. Suitable preventive measures to handle the dam problem were also analyzed and proposed.

2. RESEARCH SIGNIFICANCE

The purpose of this study was to investigate the factors that led to the failure of an earthen dam in Vietnam and to propose solutions for remediation. The case represents a common example of seepage failure resulting from the use of backfill with a lower permeability coefficient than that of the original dam material and insufficient knowledge of the geological conditions underlying the dam. Our analysis has identified effective remedial measures that could serve as a valuable reference for addressing future earth dam failures.

3. CAUSE OF THE FAILURE OF THE TRIEU THUONG 2 DAM

3.1 Description of the study site

Trieu Thuong 2, located in Trieu Thuong commune, Quang Tri, Vietnam, was constructed in 1998. The dam's potential failure could directly impact over 3,000 households and around 730 hectares of farmland and crops. Fig. 1 shows the dam's location on the map of Vietnam, along with its plan view.

The dam was constructed with 4.3 million cubic meters of homogeneous backfill soil and was initially reinforced by concrete paving slabs upstream and by planting grass downstream. Its total length measured roughly 515.6 meters, and the major dimensions of its typical cross-section upon completion in 1998 are depicted in Fig. 2.

Fig.1 Location of Trieu Thuong 2 dam on the map of Vietnam

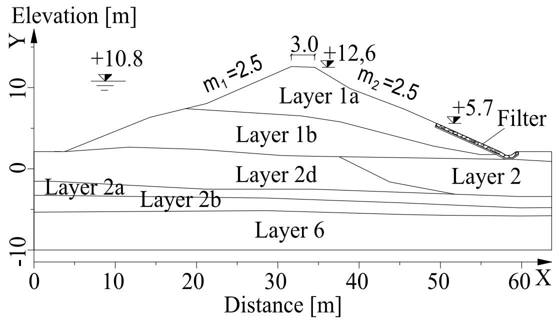

Fig.2 Typical cross-section of the dam when completed in 1989–Case 1 (elevation is in meters)

3.2 Description of the Problem of the Dam

In September 2016, the surface of the dam was expanded to a width of $B_2 = 5.0$ m, with an upstream slope coefficient of $m_1 = 2.5$ and a downstream slope coefficient of $m_2 = 2.5$. Measures were taken to improve the downstream slope, including the addition of drainage ditches, a drainage filter structure, and grass planting. A typical cross-section of the dam after the improvement in 2016 is presented in Fig. 3.

In 2016, the downstream slope of the dam experienced its first failure, triggered by heavy rainfall. The affected area was 1700 m^2 with cracks from 10 to 20 cm. The subsidence was about 60 to 80 cm from elevation + 2.0 m to elevation +10.5 m (Fig. 4a). To address the failure of the dam, only temporary remedial measures were implemented to limit the expansion of the failure area.

Bamboo piles were used to reinforce the surface slope, with a pile density of 30 cm per pile as depicted in Fig. 4b. Soil sacks were utilized to fill in all cracks and a pressure layer was constructed. A filter layer was installed downstream of the dam's toe to prevent surface water infiltration damage, along with the addition of a tarpaulin cover.

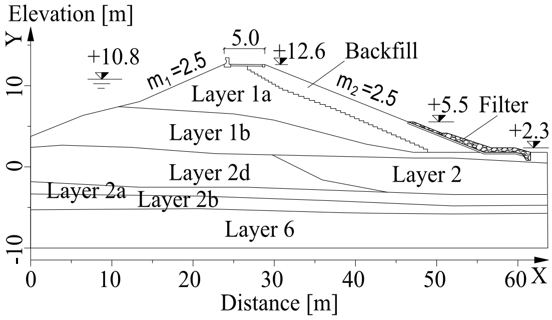

Fig.3 Typical cross-section of the dam after the improvement by adding the backfill and the filter in 2016.

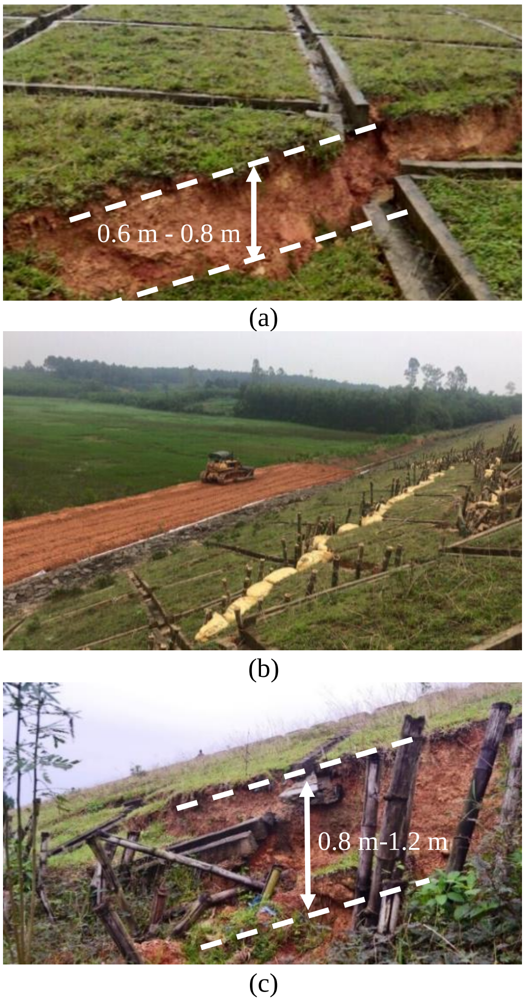

Fig.4 (a) Failure situation of the dam downstream in 2016, (b) remedial measures using bamboo piles, and (c) new crack in 2018.

During the flood season of 2017, the condition of the Trieu Thuong 2 dam worsened considerably as the sliding surface expanded by roughly 75 m in length and 30 m in width. A crack measuring between 30 cm and 50 cm wide appeared, with subsidence reaching between 120 cm and 150 cm from elevation +2.0 m to elevation +10.0 m. The sliding area totaled around 2000 m^2, as depicted in Fig. 4c. In 2018, an additional geological survey was conducted to compare treatment options before and after the rainy season. Fig. 5 shows the location of the geological surveys carried out on the downstream slope of the dam in 2018, while Fig. 6 depicts the construction of soil-cement columns intended to stabilize the dam downstream in the same year. Fig. 7 displays the stable downstream slope of the dam in 2022, four years after the improvements were made.

Fig.5 Location of the geological surveys on the downstream slope of the dam in 2018.

Fig.6 Construction of soil-cement columns to stabilize the downstream of the dam in 2018.

Fig.7 Downstream slope of Trieu Thuong 2 dam in 2022 (four years after the improvement).

4. ANALYSIS OF THE CAUSE OF THE PROBLEM

4.1 Geological Conditions and Soil Parameters

Back in 2013, surveys and assessments were conducted to improve the structure of the dam, but the investigation only covered the center of the dam, leaving the geological conditions of the site insufficiently described. In 2018, additional surveys were carried out with five more boreholes (Fig. 8). These surveys revealed the existence of a soft soil layer (Layer 2) deep beneath the downstream side of the dam, with varying thicknesses ranging from 0.8 to 4.3 meters, as shown in Fig. 9.

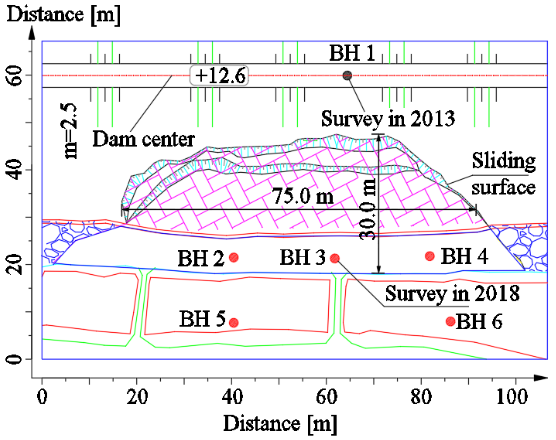

Fig.8 Plane view of geological boreholes surveyed for dam upgrading in 2013, and dam evaluation in 2018 (BH = borehole).

Characteristics of soil layers are described as follows:

Layer 1c is a dark gray rock mixed with clean gravel, with a thickness of 0.4 m. It can be found throughout the entire survey route.

Layer 1a consists of fat silt mixed with sand and fine gravel (M2S-G). It is in a solid state, with a reddish to yellow-brown color. This layer is wet and distributed throughout the survey route, with a thickness of about 1.4 m. It is the original material of the embankment.

Layer 1b is also made up of fat silt mixed with sand and fine gravel, with a semi-solid state and a reddish to yellow-brown color. It is distributed over the entire survey route, with a thickness of about 0.6 m. It is also the original material of the embankment.

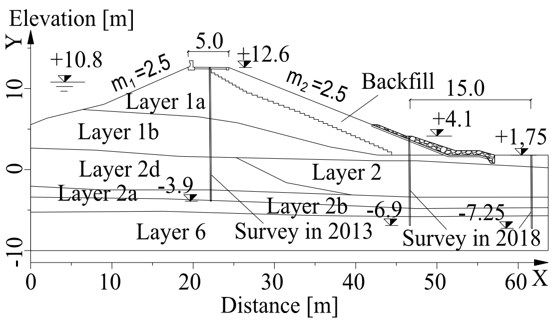

Fig.9 Cross-section showing the borehole distribution (elevation is in meters).

Layer 2 is composed of clay mixed with sand and organic matter. It is in the liquid-plastic state, with high compressibility and a dark gray color. This soft soil layer is distributed throughout the survey route, with a thickness varying from 0.8 m to 4.3 m. It originates from the old river alluvium (al.Q).

Layer 2a is made up of fat clay mixed with silt and sand, in a solid-plastic state, with medium compressibility and a dark to yellow-gray color. It is a hard soil layer distributed throughout the survey route, with a thickness of 1.5 m to 3.4 m. It originates from alluvial.

Layer 2b: This layer consists of fine-grained sandy soil mixed with silt and clay. It has a loose structure, a porous state, and is dark to yellow-gray in color. The layer is distributed throughout the survey route, with an average thickness of 1.1 m. It originates from alluvial.

Layer 2c is composed of cobbles and gravel mixed with silt and clay, with a discrete structure and a thickness ranging from 0.6 to 1.2 m. It is the old riverbed alluvial layer.

Layer 2d is clayey with high plasticity, grayish-black in color, and contains many decayed wood debris underneath. The soil has a poor structure, is soft and pliable, saturated with water, and is of alluvial origin (AI.Q).

Table. 1 Soil properties for slope stability simulation in the study area

Layer	Saturated unit weight $\frac{kN}{m^3}$	Hydraulic conductivity $\frac{m}{s}$	*Cohesion* $\frac{kN}{m^2}$	Friction angle φ (°)	E modulus $\frac{kN}{m^2}$
Backfill	21.6	1.8×10^{-7}	23.6	23.6	7000
1a	21.5	5.6×10^{-7}	23.0	17.5	7800
1b	20.0	4.5×10^{-7}	18.3	19.9	8000
2	19.4	3.2×10^{-9}	5.9	4.4	4600
2a	20.9	3.6×10^{-9}	12.5	9.7	18880
2b	21.0	3.3×10^{-7}	26.1	22.4	20000
2c	20.0	3.2×10^{-9}	26.6	20.8	11290
2d	19.2	2.9×10^{-7}	11.0	9.0	15000
5	20.4	4.2×10^{-7}	25.3	19.4	17170
6	21.0	5.0×10^{-7}	1.0	42.0	40000
SC	19.5	1.0×10^{-9}	70.0	3.4	15000

Layer 5: This layer is made up of fat silt mixed with sand and rock fragments, in a semi-solid to a solid state, with a red-brown to yellow-gray color. It originates from ruins and is a layer of rock that has completely weathered into soil particles. The layer thickness is about 1.6 m.

Layer 6: This layer is a thick bedrock layer composed of weathered siltstone. The rock is strongly weathered, but its original structure has remained intact.

Laboratory tests were used to identify the major soil parameters needed for seepage and slope stability analysis. These parameters include the unit weight, hydraulic conductivity, and shear strength. The drive-cylinder test was conducted to determine the unit weight, while both constant and falling head tests were performed to determine hydraulic conductivity. Finally, the direct shear test was applied to determine the soil's shear strength parameters. The laboratory results are presented in Table 1. The permeability coefficient of soil cement (SC) materials is 100 times smaller than that of natural soil [15].

4.2 Numerical Analyses

MIDAS GTS NX is a finite element analysis software that was developed for performing advanced geotechnical analysis of soil and rock. With MIDAS, engineers and researchers can study various phenomena such as stability, deformation, groundwater flow, and soil-structure interactions. The software was first introduced for commercial use in 1996 and has since been extensively applied in a wide range of applications [16-19].

MIDAS software is capable of modeling both steady-state and transient groundwater flow by applying Darcy's law. The steady-state flow refers to a time-independent solution where the internal and external boundary conditions remain constant. In contrast, the transient flow may exhibit different inflow and outflow with time, even if the boundary conditions are in a steady state. For this study, only the steady-state flow was considered. To analyze the seepage, the differential equation was applied.

$$\frac{\partial}{\partial x}\left(k_x\frac{\partial H}{\partial x}\right)+\frac{\partial}{\partial y}\left(k_y\frac{\partial H}{\partial y}\right)+\frac{\partial}{\partial z}\left(k_z\frac{\partial H}{\partial z}\right)+Q=\frac{\partial\Theta}{\partial t} \quad (1)$$

where: H is the total water head, k_x is the permeability coefficient in the x direction, k_y is the permeability coefficient in the y direction, k_z is the permeability coefficient in the z-direction, Q is influx/outflux per unit volume of soil per unit time, Θ is volumetric water content, and t is time.

The equation presented in Eq. 1 depicts the seepage equation applicable to transient groundwater flow. However, for steady-state flow, the right-hand side of the equation equals zero. This is because, for steady-state flow, the inflow and outflow rates through an infinitesimal volume remain constant. For soil slope stability analysis, the Mohr-Coulomb model was applied for modeling the behavior of soil layers. The strength reduction method was utilized. In this method, the shear strength parameters are continuously reduced until slope failure occurs. The theoretical equations of this kind of method are as follows:

$$C_F=\frac{C}{F_s} \quad (2)$$

$$\phi_F=tan^{-1}\left(\frac{tan\phi}{F_s}\right) \quad (3)$$

$$\tau_{fF}=C_F+\sigma tan\phi_F \quad (4)$$

where C and C_F represent the cohesion of the soil before and after the strength reduction, ϕ and ϕ_F are the internal friction of the soil before and after the strength reduction, τ_{fF} is the shear strength of soil after reduction.

4.2.1 Caculation Cases

For the targets of this study, three calculation cases were selected for the analysis: Case 1) when the dam was completed in 1989 (Fig. 2); Case 2) when the dam was improved by adding the backfill and the filter in 2016 (Fig. 3); and Case 3) when the dam was improved, and the filter structure was blocked in 2016 (Fig. 3). In all three cases, the upstream and downstream water levels are both at normal levels (+10.8 m in the upstream and +1.75 m in the downstream) in seepage analysis.

4.2.2 Boundary and Loading Condition

The MIDAS Geotechnical analysis system (GTS) software was used to conduct seepage and slope stability analysis of the downstream slope using the phi-c reduction method. For the finite element mesh, the process of creating meshes for the numerical models involved conducting multiple numerical simulations with different mesh dimensions [20-22].

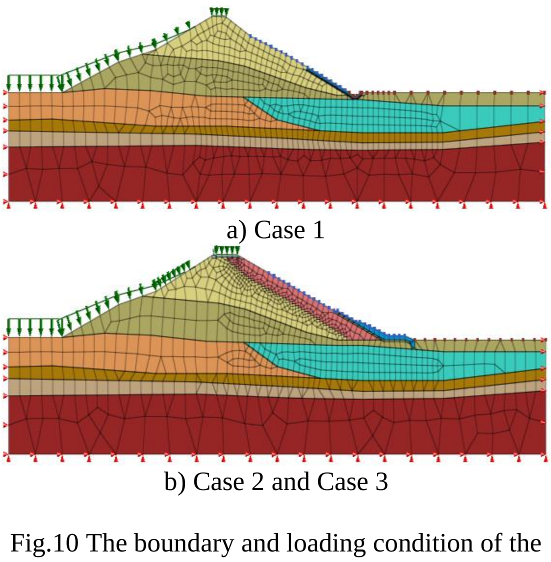

a) Case 1

b) Case 2 and Case 3

Fig.10 The boundary and loading condition of the numerical model in a) Case 1, b) Case 2 & Case 3.

To determine the optimal mesh size, the mesh dimensions were systematically reduced in each simulation until negligible changes in displacement were observed. In addition, to enhance the accuracy of the calculations, the density of triangular elements was increased near both the toe and structural interfaces. The bottom boundary of the model was fixed in both horizontal and vertical directions, as illustrated in Fig. 10, while the two sides of the model were fixed horizontally. The upstream water loading was applied to the upstream face of the dam, and the traffic loading was added to the top of the dam.

4.3 Analyses of Reducing the Phreatic Line

Fig. 11 presents the calculated results of the phreatic line within the dam body for all three cases analyzed. It should be noted that Case 3 corresponds to Case 2 with a blocked drainage system.

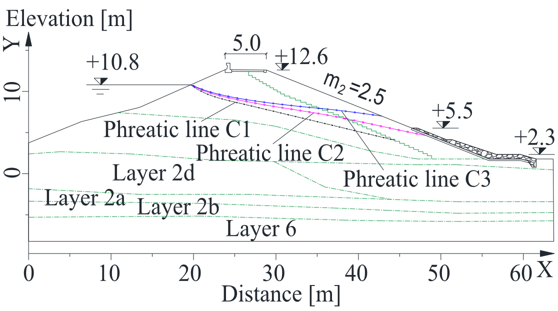

Fig.11 Phreatic lines in the dam body in Case 1 (C1), Case 2 (C2), and Case 3 (C3).

As shown in Fig. 11, the phreatic lines in all three cases rose significantly near the slope surface. This phenomenon could be attributed to several reasons: (1) during the dam upgrade and repair in 2013, the downstream embankment was filled with soil having a smaller permeability coefficient than that of the dam body; (2) the connection between the newly filled layer and the old dam body did not meet the standard, and no filter structures were installed at the contiguous position; and (3) the drainage filter structure's construction did not meet the technical requirements, resulting in its inadequate performance.

After evaluating the geological conditions and the position of the saturated line within the dam (as depicted in Fig. 11), the factor of safety (FS) for the downstream slope was simulated. The results are presented in **Fig. 12** . As can be seen, for Case 1, the FS value is 1.05. In Case 2 (after the dam underwent improvements in 2016), FS = 1.06. For Case 3 (after improvements were made and the filter layer was blocked in 2016), the FS value was calculated as 1.01. According to TCVN 8216:2009 [23], the slope's safety is questionable for all three cases, and corrective actions are necessary.

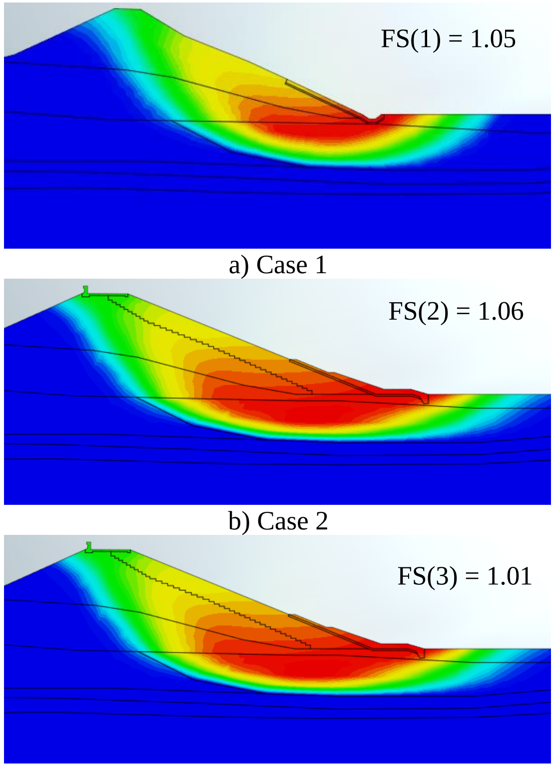

a) Case 1

b) Case 2

c) Case 3

Fig.12 Results of the stability assessment of the downstream slope of the dam, a) Case 1, b) Case 2, and c) Case 3.

5. REMEDIAL MEASURES FOR THE FAILURE OF THE DOWNSTREAM SLOPE

5.1 Selection of the Remedial Measure

The seepage analysis, stability analysis, and field survey data revealed two issues that require attention: 1) lowering the elevation of the saturated line within the dam, and 2) reinforcing the soft soil layer beneath the downstream slope. To address the seepage issue, filter layers, and drainage systems were implemented. Since soil replacement cannot be used for the soft soil layer under the downstream slope during reservoir filling due to safety requirements, a combination of soil cement mixing columns and counterweight berm was employed. Specifically, three measures were considered, as shown in Fig. 13: Case 4) a combination of stone pitching and counterweight berm, Case 5) a combination of chimney filter, stone pitching for the downstream slope, and soil-cement columns structure for the dam foundation, and Case 6) construction of a water collection filter structure at the contiguous layer, combined with ground treatment by soil-cement columns. The soil-cement column has a diameter of 800 mm, is 1.5 m apart, and is 75 m long. The water collection structure has a size of 1.0 × 1.5 m and is covered with geotextile. Typical cross-sections of the three simulated cases are presented in Fig. 13. The boundary, loading conditions of simulated cases are shown in Fig. 14.

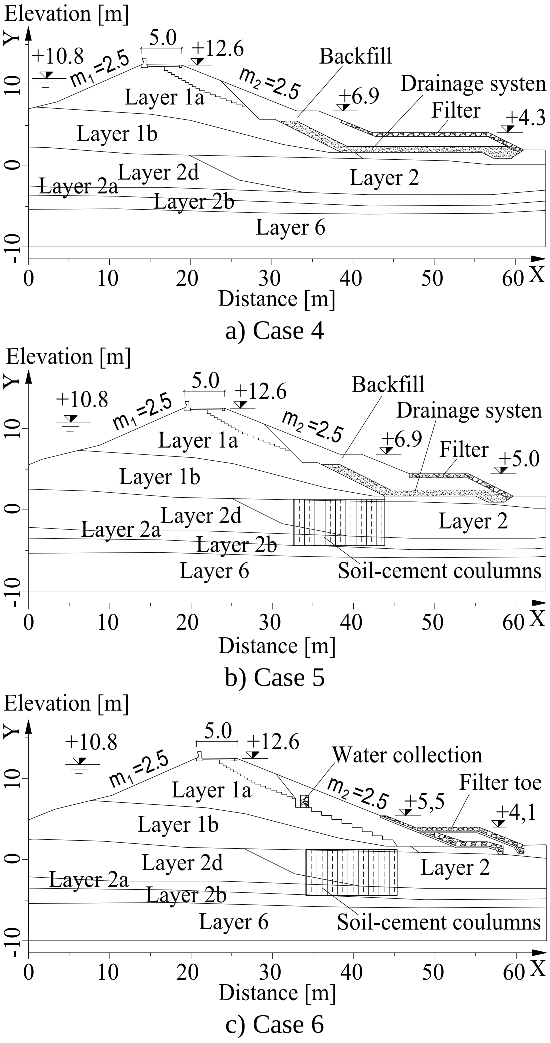

Fig.13 Typical cross-sections of the three simulated cases: Case 4, 5, and 6.

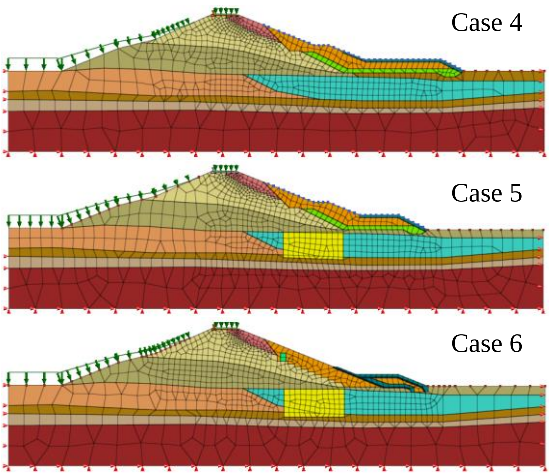

Fig.14 The boundary and loading condition of the three simulated cases: Case 4, 5, and 6.

5.2 Calculation Results and Selection of Remedial Measures

The seepage simulations for cases a, b, and c are depicted in Figures 15a, 15b, and 15c, respectively. Notably, the phreatic curves for all three cases were found to be significantly lower than those presented in Figure 11, which corresponded to the dam's completed state in 1989 and improved state in 2016. Specifically, Case 4 exhibited the lowest phreatic curve compared to Cases 5 and 6. The phreatic lines were then utilized to assess the slope stability of the dam, and the results are presented in Figures 16a, 16b, and 16c.

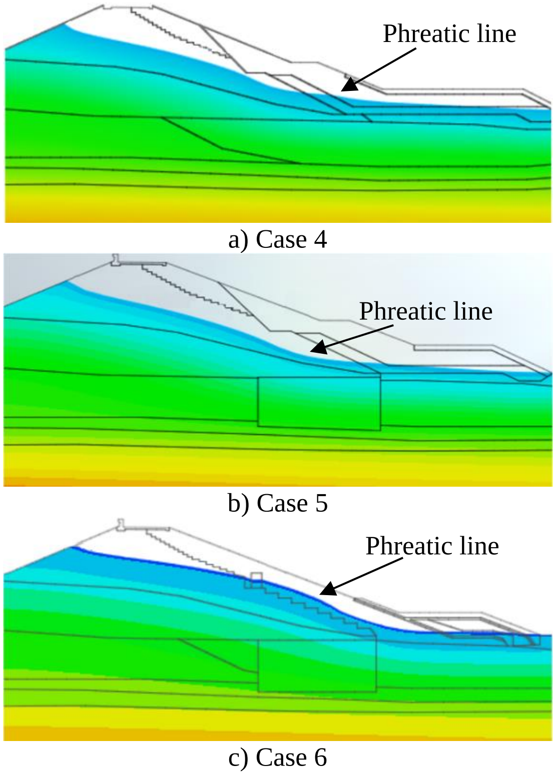

Fig.15 Results of seepage simulation for Cases 4, 5, and 6.

According to the TCVN 8216:2009 [23], the factor of safety values (FS values) for all three cases were within a safe range of stability, as depicted in Fig. 16. However, these factors of safety were not far from the threshold value ($[FS = 1.3]$ [23]). To be specific, using the strength reduction method, FS(4) = 1.08, FS (5) = 1.33, and FS(6) = 1.31.

In case 4, the FS value was the smallest. For this case, the lower phreatic curve may be attributed to the impact of the new backfill layer that compressed and damaged the soft soil layer's structure. Case 5 showed the highest factor of safety value. It might be due to the effective treatment method that lowered the phreatic line. However, this case has several drawbacks as the construction of a downstream water filter structure may lead to dam failure due to the current water storage and the impending rainy season. Therefore, Case 6 was chosen as the optimal solution to the dam failure problem.

As mentioned, Case 6 involved constructing a drainage system at the interface between the original dam surface and the new backfill and reinforcing the foundation with soil-cement columns.

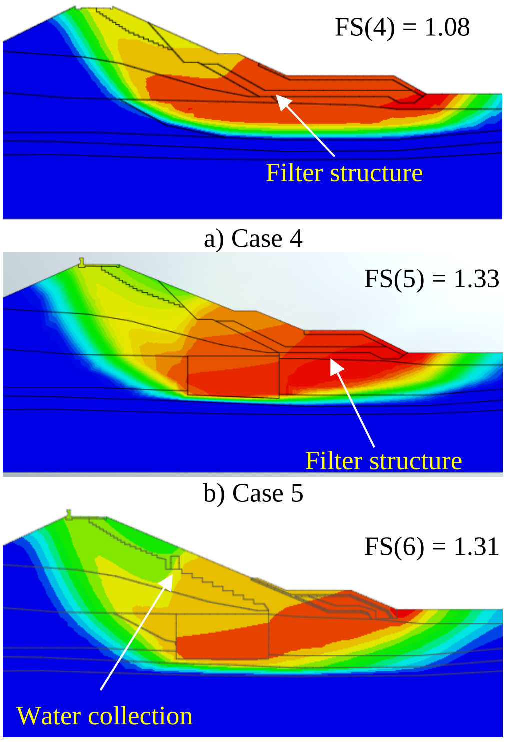

a) Case 4

b) Case 5

c) Case 6

Fig.16 Results of slope stability analyses

6. CONCLUSIONS

This article investigates the underlying causes of the failure of the downstream slope at the Trieu Thuong No.2 dam in Quang Tri, Vietnam, and proposes remedial measures to address the issue. The failure of the downstream slope was caused by several factors, including the presence of an undetected soft soil layer beneath the dam foundation during the initial design phase, a decrease in the hydraulic conductivity of the backfill when widening the embankment, leading to an elevated phreatic line within the dam, and the absence of drainage systems between the original and new dam layers, causing the phreatic surface to increase.

The solutions proposed in this study aimed to enhance soil shear strength and reduce the phreatic line. Soil-cement columns were implemented to reinforce the soil while replacing the backfill with higher hydraulic conductivity, and establishing a drainage system at the junction of the old and new layers was undertaken to achieve the latter goal. The outcome indicated that the applied measures effectively addressed the dam's seepage and stability issues.

The simulation results indicate that Case 6 was the optimal and efficient solution, effectively lowering the phreatic line and addressing seepage issues while stabilizing the soft soil layer (layer 2) to enhance overall dam stability. As of February 2023, nearly five years after the implementation of the solution, the dam remains in excellent condition.

To ensure effective upgrades and repairs of earth dams, especially when addressing issues, it is crucial to conduct a comprehensive analysis of the original design documentation, historical incident records, monitoring data, and survey data.

To facilitate future studies, it is recommended to assess the impact of uncertainties in input data, as many geotechnical inputs involve some level of uncertainty in conducting slope stability analyses. Also, it is advisable to conduct a thorough parametric analysis to determine the efficacy of remedial measures in addressing slope instability.

7. REFERENCES

[1] Sharma R., and Manna B., Failure analysis of homogeneous earthen dam, in Indian Geotechnical Conference 2019, S. Patel, et al., Editors. 2021, Springer, Singapore: India, 2019, pp. 829-837.

[2] Umaru A.B., Sangodoyin A.Y., and Oke I.A., On the causes and effects of earth dams failures in North-Eastern Nigeria. International Journal of Engineering Research & Technology, Vol. 3, Issue 2, 2014, pp. 2978-2985.

[3] Aribawa T.M., Saroni S., Idham R.M., Yeremia I.S., Akbar R., Mohammad F., Assessment of flood propagation due to several dams break in Banten province. International Journal of GEOMATE. Vol. 20, 2021, pp. 185-190.

[4] Lukman S., Otun J.A., Adie D.B., Ismail A., Oke I.A., A brief assessment of a dam and its failure prevention. Journal of Failure Analysis and Prevention., Vol. 11, 2010, pp. 97-109.

[5] Kolala M., The causes of dam failures a study of earthen embankment dams on the Copperbelt province of Zambia. International Journal of Engineering Research & Technology, Vol. 4, Issue 2, 2015, pp. 301-309.

[6] Saluja IS, Athar M., and Ansari S.A., Causes of failure of earthen dams and suggested remedial measures. International Journal of Engineering Technology Science and Research. Vol 5, Issue 3, 2018, pp. 177-185.

[7] Arora K.R., Irrigation Water Power and Water Resources Engineering. Delhi: Standard Publisher Distributors, 2002, pp. 1-1105.

[8] Zhang L.M., Xu Y., and Jia J.S., Analysis of earth dam failures - A database approach. Georisk: Assessment and Management of Risk for Engineered Systems and Geohazards. Vol. 3, Issue 3, 2009, pp. 184-189.

[9] Mahmood N.S., Rafid A., Sadeq O.S., Nadhir A.A., Seepage Problem Through the Foundation f a Spillway with Selected Treatment Methods. Mathematical Modelling of Engineering Problems, Vol. 9, Issue 3, 2022, pp. 819-824.

[10] Fadaei-Kermani E., Shojaee S., Memarzadeh R., Barani G. A., Numerical simulation of seepage problem in porous media. Applied Water Science. Vol. 9, Issue 79, 2019, pp. 1-8.

[11] Pham Q.D., Tran T.V., and Trinh M.T., Relation between the plasticity index and key consolidation parameters of soft ground stabilized by vacuum preloading together with vertical drains. International Journal of GEOMATE.Vol.18, Issue 69,2019, pp. 224-229.

[12] Tran D.Q., Shinichi N., Masateru S., Tatsuro N., Research on cause of dam failure from viewpoint of hydraulic fracturing – case study of a dam failure in Vietnam. International Journal of GEOMATE. Vol.14, Issue 41,2018, pp.86-94.

[13] Aga A.G., Embankment dam seepage and slope stability analysis: The case of Arjo-dedessa Dam, Ethiopia. Journal of Civil, Construction and Environmental Engineering. Vol. 6, Issue 4, 2021, pp. 104-109.

[14] Punmia B.C., Lal P.B.B., Irrigation and Water Power Engineering. India: Laxmi Publications (P) Ltd, 1992, pp. 1-981.

[15] Vietnam Academy for water resources., Hydraulic structures - Cement soil columns created by Jet-grouting method - Technical requirement for design, construction and acceptance in the soft ground reinforcement. Ministry of Science and Technology: Ha Noi, 2015, pp. 1-30.

[16] Chen S., Yang Z., Zhang W., Li L., Zheng Y., Yuan Y., Numerical simulation of the stability of a cutting slope and study on its reinforcement scheme. Hindawi Advances in Civil Engineering, Vol. 2022, 2022, pp. 1-14.

[17] Velychko S., and Dupliak O., Assessment of the influence of mountain flood control reservoir operation on the floodplain stability during an extreme flood. Ecol. Eng. Environ. Technol, Vol. 22, Issue 1, 2021, pp. 31-38.

[18] Banerjee L., and Chawla S., A finite element approach of stability analysis of over burden dump slope - A case study, in Proceedings of the Indian Geotechnical Conference GeoNEst 2017, IIT Guwahati, India, 2017, pp. 14-17.

[19] Ahmad M., and Richard R., Comparison between Ramberg-Osgood and Hardin-Drnevich soil models in Midas GTS NX. Pollack Periodica, Vol. 16, Issue 3, 2021, pp. 1-6.

[20] Maleki M., Khezri A., Nosrati M., Hosseini S. M. M. M., Seismic amplification factor and dynamic response of soil-nailed walls. Modeling Earth Systems and Environment, Vol. 9, 2023, pp. 1181–1198.

[21] Maleki, M., and Nabizadeh A., Seismic performance of deep excavation restrained by guardian truss structures system using quasi-static approach. Applied Sciences, Vol. 3, Issue 414, 2021, pp. 1-17.

[22] Maleki M., Hosseini SMMM, Assessment of the Pseudo-static seismic behavior in the soil nail walls using numerical analysis. Innovative Infrastructure Solutions, Vol. 7, Issue 262, 2022, pp. 1-18.

[23] Vietnam Design standard for compacted earth dam TCVN 8216:2009. Vietnam Ministry of Science and Technology: Ha Noi, 2009, pp. 1-10.